ON THE SHADOW EFFECT IN HIGH ENERGY SCATTERING FROM DEUTERONS

E.S. Abers [+], H. Burkhardt [*], V.L. Teplitz [×]

and

C. Wilkin [‡]

CERN - Geneva

A B S T R A C T

Most of the experimental information on high-energy scattering from neutrons has been obtained by comparing cross-sections from protons and deuterons. The extraction of neutron cross-sections from such data is non-trivial: the most widely used model is the semi-classical ray formula of Glauber, which gives, in addition to the impulse approximation terms, a shadow correction due to the mutual "eclipsing" of the nucleons in the deuteron.

In this paper we show that if the nucleon-nucleon scattering amplitudes near the forward direction can be represented as sum of Regge Poles, the shadow term that Glauber includes vanishes rapidly at high energies but that other terms remain which provide a somewhat smaller shadow effect.

We first give a diagrammatic derivation of the Glauber formula and show that his shadow term, which comes from the diagram where both nucleons interact with the incident fast particle, does not in fact have the Regge cut necessary for its persistence at high energies. We then show that certain diagrams with inelastic virtual states between the two interactions do have such cuts and we express their contribution in terms of a partial inelastic cross-section and a statistical factor. An experimental clarification can only be achieved by accurate experiments with high energy neutron beams.

[+] National Science Foundation postdoctoral fellow.
Present address : U.C.L.A., Los Angeles, Calif.

[*] On leave of absence from the Department of Mathematical Physics, University of Birmingham.

[×] NATO postdoctoral fellow.
Present address : M.I.T., Cambridge, Mass.

[‡] Present address : Brookhaven National Laboratory, Upton, L.I., N.Y.

65/1341/5-TH.602
10 September 1965

I. INTRODUCTION

The vast majority of our experimental information about scattering processes which involve neutrons has been obtained from a detailed comparison of the scattering from deuterons with that from protons, a process which has been aptly described as "a complicated piece of hieratic lore" [1]. The basic problem is the estimation of the so-called "shadow" or "eclipse" effect, which is the reduction of the deuteron cross-sections below the sum of the cross-sections for scattering from the individual nucleons. This arises because the nucleons, being bound together, hide behind each other part of the time and are thus partly screened from the incident particle flux.

Many years ago, Glauber [2] made an evaluation of this correction term which was both intuitively sensible and well checked at moderate energies, and which has since then been universally used in practice. It is the aim of this paper to re-examine the Glauber eclipse term, paying particular attention to the high energy limit. Although we shall confine ourselves to the case in which the target is a deuteron, and where the nucleon amplitudes, at least near the forward direction, can be represented by a Regge-type behaviour, the problem is really more general and we believe that the same principle can be applied to scattering from more complicated nuclei as well.

The original derivation of Glauber, which is based on the optical or eikonal approach to high energy scattering, leads in its simplest form to a cross-section for the scattering of particle x on a deuteron given by

$$\sigma_{xd} = \sigma_{xp} + \sigma_{xn} - \sigma_{xp}\sigma_{xn}\frac{\langle r^{-2}\rangle}{4\pi} \qquad (I.1)$$

where σ_{ab} is the total cross-section for ab scattering and $\langle r^{-2}\rangle$ is the average value of the inverse square separation of the nucleons in the deuteron. Udgaonkar and Gell-Mann [3] evaluated the Glauber correction

for a form of the nucleon-nucleon scattering amplitude given by one Regge pole exchange and obtained a shadow term that vanished only very slowly, as $1/\log E$, at high energies. It is shown in Section II that this approach is equivalent to calculating a certain class of field theoretic diagrams by using an approximation to the unitarity relation. However, arguments are presented in Section III which demonstrate that if off-mass-shell effects are taken into account in the intermediate states, then the result of Udgaonkar and Gell-Mann is incorrect, and the shadow term should decrease very fast with energy, like $E_L^{2\alpha(\infty)-2}$, where $\alpha(t)$ is the leading Regge trajectory at infinity. The mechanism of this cancellation is exactly that which was used by Mandelstam [4] to show that the cuts in the angular momentum plane proposed by Amati, Fubini and Stanghellini [5] were spurious. Mandelstam, however, went further and found a set of graphs which do exhibit a cut structure and in Section IV we show that the sum of such a class of diagrams leads to shadowing which, after an initial rise, again only decreases logarithmically with energy.

Our expression for the eclipse term (IV.10) is not as simple a "Golden Rule" as (I.1). In addition to containing factors which can be taken from experiment, the formula also involves others which must be estimated from theory.

Section V contains an analysis of the present experimental situation and the light it throws on this question. While the evidence is somewhat scanty, it seems to support the existence of a fairly constant shadow term up to the highest available energies, consistent with our results.

A summary of the main results is to be found in Section VI together with suggestions for both experimental and theoretical work which will help to clarify the problem further.

II. SEMI-CLASSICAL THEORY OF THE ECLIPSE TERM

The semi-classical ray model of Glauber [2] is both a simple and intuitively appealing approximation to the scattering of a fast particle by a deuteron, given the amplitudes for the scattering by the proton and neutron individually. Roughly, the model supposes that the scattering from the individual nucleons can be described by the change of phase $\delta_{p,n}(\vec{b})$ of the projectile's wave front at each point $\vec{b}$ in the plane perpendicular to the wave front. Since $|\vec{b}|$ is the impact parameter, equal to ℓ divided by the projectile momentum, then $\delta_{p,n}(\vec{b})$ is just the phase shift of the ℓ^{th} partial wave. It is assumed that $\delta_d(\vec{b})$ for scattering from the deuteron is just the sum of the phase shifts from the individual nucleons $\delta_p(\vec{b}_p)+\delta_n(\vec{b}_n)$, where $\vec{b}_p$ and $\vec{b}_n$ are the (two-dimensional) vector distances between $\vec{b}$ and the proton and neutron positions, respectively. The result has to be averaged over the probability distribution over the nucleons which is described by the deuteron wave function.

The result contains three terms [see Eq. (II.5)]. The first two are just the impulse approximation for scattering from one of the nucleons while the second remains a "spectator". The third term is the eclipse or shadow term and may be thought of as a correction due to the non-zero probability that one nucleon is hidden behind the other and cannot then interact with the incident particle.

Udgaonkar and Gell-Mann [3] used a form of the Glauber model at high energies, taking for the amplitudes for scattering by the individual nucleons the exchange of the vacuum trajectory. We want now to discuss this method in terms of a certain class of diagrams.

Let us first write down the general result of Glauber's model in the notation of UCM. For simplicity we consider all the particles to be scalars. If we assume that the nucleons have a common mass M, then the masses involved are M_d, M, M_x and the deuteron binding energy $B = 2M-M_d$, where x will always refer to the fast immigrant particle: s and t are the energy and momentum transfer variables in either xN or xd scattering.

Let $\psi(\vec{r})$ be the normalized deuteron wave function, where $\vec{r}$ is the separation between the neutron and proton. The momentum space wave function

$$\phi(\vec{p}) = \frac{1}{(2\pi)^{3/2}} \int d^3\vec{r}\, \psi(\vec{r})\, e^{-i\vec{p}\cdot\vec{r}} \qquad \text{(II.1)}$$

is also normalized to unity and describes the amplitude for momentum $\vec{p}$ of the proton or neutron. Following UGM we define the deuteron form factor

$$G(p^2) \equiv \int d^3\vec{r}\, |\psi(\vec{r})|^2\, e^{i\vec{p}\cdot\vec{r}} = \int d^3q\, \phi(\vec{p}-\vec{q})\, \phi(\vec{q}) \qquad \text{(II.2)}$$

We normalize our scattering amplitudes such that

$$\frac{d\sigma}{dt} = |F(s,t)|^2 \qquad \text{(II.3)}$$

The optical theorem becomes

$$\sigma^T(s) = 4\sqrt{\pi}\, \mathrm{Im}\, F(s,0) \qquad \text{(II.4)}$$

For a given velocity of the projectile x, the centre-of-mass energy squared is s_{xd} or s_{xp}. In the rest system of the deuteron, compared to the particle x, the deuteron and the nucleons it contains are both at rest, and so in the high energy limit $s_{xp} = s_{xn} = \frac{1}{2}s_{xd}$. The result of Glauber's analysis is

$$F_{xd}(s,t) = G(-t/4)\left[F_{xp}(s_{xp},t) + F_{xn}(s_{xn},t)\right] - \frac{i}{(2\pi)^{3/2}} \int G(p^2)\, F_{xp}\left[s_{xp}, -\left(\frac{\vec{q}}{2}+\vec{p}\right)^2\right] F_{xn}\left[s_{xn}, -\left(\frac{\vec{q}}{2}-\vec{p}\right)^2\right] d^2\vec{p} \qquad \text{(II.5)}$$

where $q^2 = -t$ and the angle of the two-dimensional vector $\vec{q}$ is the azimuth of the scattering: the integration d^2p is also over the plane perpendicular to the incident direction. It can readily be seen by using the optical theorem that the eclipse term reduces the scattering.

$$\sigma_{xd}^T = \sigma_{xp}^T + \sigma_{xn}^T - \frac{2}{\pi} \mathrm{Re} \int G(p^2) F_{xp}(s,-p^2) F_{xn}(s,-p^2) d^2p \quad \text{(II.6)}$$

where we have used the condition $G(0) = 1$. The simple formula (I.1) is obtained from (II.6) by making the dubious approximations that the amplitudes $F_{\substack{xp \\ xn}}$ are purely imaginary and that the amplitudes are not rapidly varying over the range of integration which is allowed by $G(p^2)$. We can then take them out of the integral to obtain

$$\begin{aligned} \sigma_{xd}^T &= \sigma_{xp}^T + \sigma_{xn}^T - \frac{1}{8\pi^2} \sigma_{xp}^T \sigma_{xn}^T \int G(p^2)\, d^2p \\ &= \sigma_{xp}^T + \sigma_{xn}^T - \frac{1}{4\pi} \sigma_{xp}^T \sigma_{xn}^T \langle r^{-2} \rangle \end{aligned} \quad \text{(II.7)}$$

where $\langle r^{-2} \rangle = \frac{1}{2\pi} \int G(p^2) d^2p$ represents the average inverse square separation of the particles in the deuteron. We shall sometimes use this formula in the equivalent form

$$\sigma_{xd}^T = \sigma_{xp}^T + \sigma_{xn}^T - 4 \sqrt{\left(\frac{d\sigma_{xp}}{dt} \right)_{t=0}^{el} \left(\frac{d\sigma_{xn}}{dt} \right)_{t=0}^{el}} \cdot \langle r^{-2} \rangle \quad \text{(II.8)}$$

The result of UGM is obtained by writing

$$F_N(s_{xN}, t) = \frac{i}{4\sqrt{\pi}} \sigma_N^T B_N(t) \left(\frac{s}{s_0} \right)^{\alpha(t)-1} \quad \text{(II.9)}$$

where $B_N(0) = 1$.

We now write down dispersion diagrams corresponding to the terms of (II.5). The impulse approximation corresponds to Fig. 1

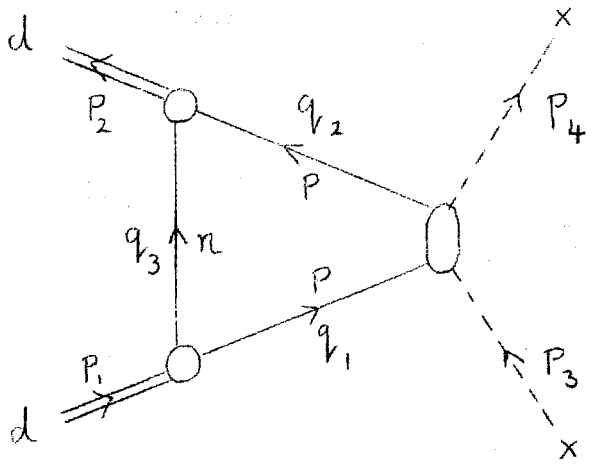

Fig. 1

together with the same diagram with the neutron and proton interchanged. The eclipse term is due to processes where x scatters first off one nucleon and then off the second, i.e., to Fig. 2 :

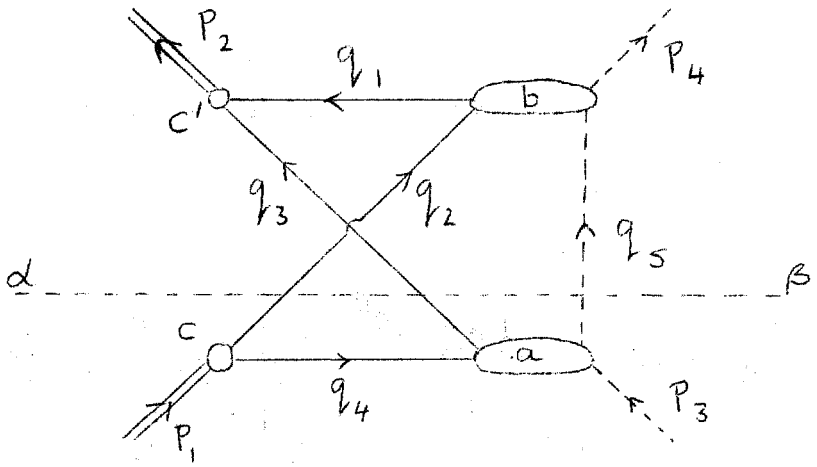

Fig. 2

There are contributions from two such diagrams. In the first q_3 and q_4 are protons, in the second they are neutrons.

To write down analytic expressions for these diagrams, we must know the nucleon amplitudes $F_{xN}(s_{xN}, t_{xN})$ which we have indicated by "blobs" a and b and the deuteron vertex function c and c'. In order not to be confused with extraneous complications, we take the deuteron-nucleon vertex to be a point interaction of the type $g\phi^3$ and then compare with the wave function picture by adjusting the coupling constant g so that the residue of the deuteron pole in n-p scattering is correct. With our definition of g, the amplitude for n-p scattering near the deuteron pole is

$$F_{np}(s,t) = -\frac{g^2}{4\sqrt{\pi}\, M_d^2 (s - M_d^2)} = \frac{g^2}{16\sqrt{\pi}\, M_d^2 (\vec{p}^2 + \alpha^2)} \qquad \text{(II.10)}$$

However, this quantity may also be calculated from wave mechanics. If at large separations r,

$$\psi(\vec{r}) = \frac{N e^{-\alpha r}}{\sqrt{4\pi}\, r} \qquad \text{(II.11)}$$

where $\alpha^2 = MB$, the momentum space wave function is from (II.1)

$$\phi(\vec{p}) = \frac{\sqrt{4\pi}\, N}{(2\pi)^{3/2} (\vec{p}^2 + \alpha^2)} \qquad \text{(II.12)}$$

plus terms regular at $p^2 = -\alpha^2$. It then follows from effective range theory for potential scattering [6] that near the pole

$$F_{np} = -\frac{2 N^2 \pi^{3/2}}{M_d (\vec{p}^2 + \alpha^2)} \qquad \text{(II.13)}$$

To order B/M_d, we may therefore identify

$$\frac{g^2}{4\pi} = 8 N^2 M_d \qquad \text{(II.14)}$$

and whenever the combination

$$\frac{g}{\sqrt{8M_d(2\pi)^3}\ (\vec{p}^{\,2}+\alpha^2)} \tag{II.14'}$$

occurs in the evaluation of the diagrams, it is to be replaced by $\phi(\vec{p})$. This is clearly correct in so far as only the tail of the deuteron wave function is important, and will suffice for our purposes [7].

Finally, it is convenient to replace F by invariant amplitudes A which can be computed from crossing symmetric Feynman rules and which satisfy a simple unitarity condition. Thus, let $\langle m|S|n\rangle$ be the S matrix element between initial and final states containing n and m distinguishable particles, normalized to products of delta functions in momentum space. Then define $\langle m|A|n\rangle$ by

$$\langle m|S|n\rangle = \langle m|n\rangle + 2i\frac{\delta^4(\sum p_m - \sum p_n)\langle m|A|n\rangle}{\sqrt{\prod_{i=1}^{m+n}(2E_i)}} \tag{II.15}$$

where p_i is the four-momentum of the i^{th} external particle. The contribution to $\mathrm{Im}\,A$ due to ℓ-particle intermediate states is

$$\mathrm{Im}\langle m|A|n\rangle = \int d\tau_1 \cdots d\tau_\ell\ \delta^4\Big(\sum_{i=1}^{\ell} p_i\Big)\langle \ell|A|m\rangle^*\langle \ell|A|n\rangle \tag{II.16}$$

where $d\tau_i = d^3p_i/2E_i$. For two-particle elastic scattering, A is related to the previously defined F by

$$F(s,t) = \frac{(2\pi)^{3/2}}{s}\,A(s,t) \tag{II.17}$$

After these preliminaries, we can now write down the contributions to $A_{xd}(s,t)$ from the process described by Fig. 1. This is

$$A^{(p)}_{xd}(s,t) = \frac{i g^2}{(2\pi)^4} \int \frac{d^4 q_3 \, A_{xp}(s_a, t)}{[q_3^2 - m^2 + i\varepsilon][q_1^2 - m^2 + i\varepsilon][q_2^2 - m^2 + i\varepsilon]} \qquad \text{(II.18)}$$

where A_{xp} is the x-proton amplitude, slightly off the mass shell and $s_a = (p_3 + q_1)^2$. Consider first the integral over E_3. The original integration contour lies along the whole real axis, but we want to deform this into the upper half plane and then discard the contribution from the infinite semi-circle. In so doing, we encounter cuts due to the q_1^2 and q_2^2 denominators, from $A_{xp}(s_a,t)$ and in more realistic models, from the deuteron-nucleon vertices. In addition, there is a simple pole at $E_3 = \sqrt{m^2 + \vec{q}_3^{\,2}} - i\varepsilon$. Now several authors [8),9),10)] have shown that the impulse approximation at high energies corresponds to ignoring all the singularities except this pole, that is, doing the replacement

$$\frac{1}{q_3^2 - m^2 + i\varepsilon} = -\frac{i\pi}{E_3} \, \delta\left(E_3 - [m^2 + \vec{q}_3^{\,2}]^{1/2}\right) \qquad \text{(II.19)}$$

To continue, let us work in the Breit system defined by

$$\begin{aligned} P_1 &= \left[M_d + q^2/8M_d \, , \, -\vec{q}/2 \right] \\ P_2 &= \left[M_d + q^2/8M_d, \; \vec{q}/2 \right] \\ P_3 &= \left[\omega \, , \, \frac{\vec{q}}{2} + \vec{P}_3 \right] \\ P_4 &= \left[\omega \, , \, \frac{\vec{q}}{2} - \vec{P}_3 \right] \end{aligned} \qquad \text{(II.20)}$$

with $\vec{p}\cdot\vec{q} = 0$ and $\vec{p}$ along the z axis. Along this axis, the deuteron momentum both before and after is zero and the projectile's momentum does not change. Using the restriction imposed by the energy delta function, we see that, to order B/M,

$$q_2^2 - M^2 = 2\left[\left(\vec{q}_3 + \vec{q}/4\right)^2 + \alpha^2\right]$$

and

$$q_1^2 - M^2 = 2\left[\left(\vec{q}_3 - \vec{q}/4\right)^2 + \alpha^2\right] \qquad \text{(II.21)}$$

In the same approximation, we set $E_3 = M$ in the denominator to obtain [using (II.14')]

$$A_{xd}^{(p)}(s,t) = \frac{q^2}{64\pi^3 M}\int \frac{d^3q_3\, A_{xp}(s_a,t)}{\left[\left(\vec{q}_3+\vec{q}/4\right)^2+\alpha^2\right]\left[\left(\vec{q}_3-\vec{q}/4\right)^2+\alpha^2\right]}$$

$$= \frac{8M_d(2\pi)^3}{64\pi^3 M}\int d^3q_3 A_{xp}(s_a,t)\,\phi\left(\vec{q}_3-q/4\right)\phi\left(\vec{q}_3+q/4\right) \qquad \text{(II.22)}$$

In the high energy, low momentum transfer region that we are interested in ($\omega \to \infty$, q^2 small), s_a approaches $s/2$ for all q_3, so that we may use (II.2) to obtain the final result

$$A_{xd}^{(p)}(s,t) = 2\,A_{xp}(s,t)\,G(q^2/4)$$

or

$$F_{xd}^{(p)}(s,t) = F_{xp}(s,t)\,G(-t/4) \qquad \text{(II.23)}$$

An identical computation, with n and p interchanged, gives the second term of (II.5).

In this analysis of the impulse approximation, there is the explicit assumption that the deuteron is a bound state in the n-p channel, effectively uncoupled from all other channels, e.g., n-p-π. This is plausible because the binding energy in the former case is 2 MeV, whereas it is ~140 MeV in the latter. Nevertheless, it is an assumption and there appears no way of ruling out a small effect from multi-channel processes. If the deuteron can exist virtually in other states, then the d-p-n form factor (II.2) satisfies the condition $G_{pn}(0) < 1$. Consequently, if $\sigma^{T}_{xN} > \sigma^{T}_{xN\pi}$, the impulse approximation gives an overestimate for σ^{T}_{xd} which might mistakenly be interpreted as shadowing.

Returning to the eclipse diagram, (Fig. 2), we must now ask what physical approximations correspond to the wave function picture which is responsible for Eq. (II.5). The Glauber method envisages a two-stage process in which the x particle first scatters off the proton, say, and then off the neutron. In terms of diagram, Fig. 2, only those contributions are taken into account in which the lines q_2, q_3 and q_5 are real intermediate states. We are therefore led to keep only those contributions to Fig. 2 which arise from calculating $A^{(e)}_{xd}(s,t)$ by using three-particle unitarity, cutting along $\alpha\beta$.

Using this approach we shall obtain a form for the eclipse term, $\mathrm{Im}\, A^{(e)}_{xd}(s,t)$, very similar to the Glauber form (II.5). Our expression (II.32) agrees exactly for purely imaginary xN amplitudes, but the real parts of these increase the shadowing in contradistinction to (II.5). We are inclined to believe that the generalized unitarity approximation gives a more reliable method of computing these reactive effects but, as the effect of the real parts is small in the high energy region, we shall leave this interesting difference for later consideration. In view of its very similar physical content, we shall call (II.32) the 'Glauber' formula.

We must now study $2 \leftrightarrow 3$ body amplitudes, for example $p_1+p_3 \to q_2+q_3+q_5$. In terms of the two-body amplitudes these are given by

$$A_{xd\to xnp} = \frac{g}{(2\pi)^{3/2}} \frac{A_{xp}(s_a, t_a)}{(q_1^2 - M^2)} \qquad \text{(II.24)}$$

$$A_{xnp\to xd} = \frac{g}{(2\pi)^{3/2}} \frac{A_{xn}(s_b, t_b)}{(q_4^2 - M^2)} \qquad \text{(II.24')}$$

where

$$s_a = (q_3+q_5)^2 \,, \quad t_a = (p_3-q_5)^2$$
$$s_b = (q_2+q_5)^2 \,, \quad t_b = (p_4-q_5)^2 \qquad \text{(II.25)}$$

which, in the high energy limit, become $s_a = s_b = s/2$. Combining these two amplitudes by the unitarity rule (II.16), we obtain

$$\mathrm{Im}\, A^{(e)}_{xd}(s,t) = -\frac{g^2}{(2\pi)^3} \int d\tau_2\, d\tau_3\, d\tau_5\, \delta^4(q_2+q_3+q_5-p_1-p_3) \qquad \text{(II.26)}$$
$$\times \frac{A_{xp}(s_a, t_a)}{(q_4^2 - M^2)} \frac{A^*_{xn}(s_b, t_b)}{(q_1^2 - M^2)}$$

We now write $d\tau_5 = d^4q_5\, \delta(q_5^2 - M^2)$ and use the four-dimensional delta function to eliminate the q_5 integration. We also use the same reference frame as before (II.20), together with the kinematic relations

$$q_1^2 - M^2 = -2\left[(\vec{q}_1 - \vec{q}/4)^2 + \alpha^2\right]$$
$$q_4^2 - M^2 = -2\left[(\vec{q}_4 + \vec{q}/4)^2 + \alpha^2\right] \qquad \text{(II.27)}$$

to write

$$\mathrm{Im}\, A^{(e)}_{xd}(s,t) = -\frac{g^2}{32\pi^3}\int \frac{d^3q_2}{2E_2}\frac{d^3q_3}{2E_3}\,\delta(q_5^2-M_x^2) \times \frac{A_{xp}(s_a,t_a)}{[(\vec{q}_4+\vec{q}/4)^2+\alpha^2]}\,\frac{A^*_{xn}(s_b,t_b)}{[(\vec{q}_1-\vec{q}/4)^2+\alpha^2]} \qquad \text{(II.28)}$$

Next we change the integration variable d^3q_2 to d^3p where $p = q_3+q_2$; then $t_a = (p_1-p)^2$, $t_b = (p_2-p)^2$. Since in this system $|\vec{q}| \ll M$, the integrand can only be large when $|\vec{q}_1|, |\vec{q}_4| \ll M$ and hence when $|\vec{q}_2|, |\vec{q}_3| \ll M$. But this also requires that $|\vec{p}| \ll M$ too. We make errors only of the order q^2 or B/M if we set $E_1 = E_2 = E_3 = E_4 = M$ in the integrand. In this approximation

$$t_a = -(\vec{q}/2 - \vec{P})^2$$

$$t_b = -(\vec{q}/2 + \vec{P})^2 \qquad \text{(II.29)}$$

while the amplitude becomes

$$\mathrm{Im}\, A^{(e)}_{xd}(s,t) = \frac{-1}{M}\int d^3p\, G(p^2)\,\delta\left[\frac{s}{M_d}(M_d - p_0 - p_z)\right] \times A_{xp}\left(\frac{s}{2}, -(\vec{q}/2-\vec{P})^2\right) A^*_{xn}\left(\frac{s}{2}, -(\vec{P}+\vec{q}/2)^2\right) \qquad \text{(II.30)}$$

which, after the final integration over the delta function, reduces to

$$\mathrm{Im}\, A^{(e)}_{xd}(s,t) = \frac{-2}{s}\int d^2p\, G(p^2)\, A_{xp}\left(s/2, -(\vec{q}/2-\vec{P})^2\right) \times A^*_{xn}\left(s/2, -(\vec{q}/2+\vec{P})^2\right) \qquad \text{(II.31)}$$

We must finally add the contribution of the diagram in which the neutron and proton are interchanged and this gives the complex conjugate contribution so that we are led back to the 'Glauber' formula for the shadow term

$$\mathrm{Im}\, F_{xd}^{(e)}(s,t) = \frac{-1}{(2\pi)^{3/2}}\, \mathrm{Re} \int d^2p\; G(p^2)\, F_{xp}\left(\frac{s}{2}, -\left(\frac{\vec{q}}{2}+\vec{p}\right)^2\right) \times F_{xn}^{*}\left(\frac{s}{2}, -\left(\frac{\vec{q}}{2}-\vec{p}\right)^2\right) \quad \text{(II.32)}$$

The UGM model, which assumes that the proton and neutron amplitudes are dominated by Regge poles, is obtained by substituting (II.9) into (II.32)

$$\mathrm{Im}\, F_{xd}^{(e)}(s,t) = -\frac{\sigma_p\, \sigma_n}{8\pi^2}\, \mathrm{Re} \int d^2p\, G(p^2)\, B\left(-(\vec{p}-\vec{q}/2)^2\right) \times B\left(-(\vec{p}+\vec{q}/2)^2\right) \times \left(\frac{s}{s_0}\right)^{\alpha\left[-(\vec{q}/2-\vec{p})^2\right]+\alpha\left[-(q/2+\vec{p})^2\right]-2} \quad \text{(II.33)}$$

Since there is an integration over the arguments of the Regge trajectories, the shadow term corresponds to a Regge cut [4),5)], whose leading branch point is at

$$l = 2\,\alpha\,(t/4) - 1 \quad \text{(II.34)}$$

III. ASYMPTOTIC BEHAVIOUR OF THE GLAUBER TERM

It has been shown in the previous Section that Fig. 2, which corresponds to the Glauber shadow term, is just the graph in which UGM found cuts in the angular momentum plane. As was pointed out, the approximation to Fig. 2, which gives just the UGM result, involved the use of three-particle unitarity in a channel whose energy gets very large. Such a procedure has been shown by Mandelstam [4] to be very dangerous, since there are other contributions to the imaginary part from multi-particle unitarity cuts, which sometimes induce a cancellation of the Regge cut. If the Regge pole is represented as a sum of ladder diagrams [11], for example, then one such contribution comes from cutting along AB in Fig. 3

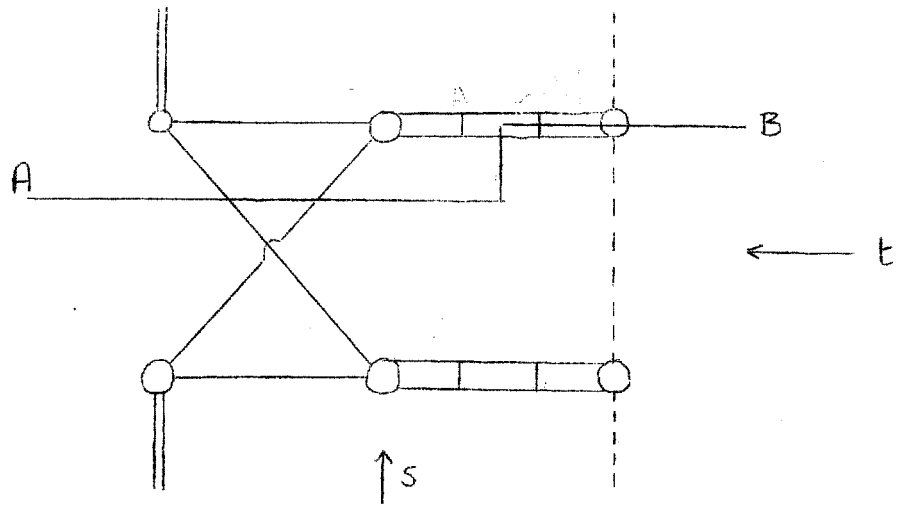

Fig. 3

UGM have speculated that nevertheless the Regge cut displayed in (II.33) is present in this process as a consequence of the anomalous thresholds which occur because of the small binding energy of the deuteron. A proof that the cut in this diagram is spurious has been given by one of us [12]; we give here an outline of this argument from which it will be clear that even with anomalous thresholds the eclipse diagram (Fig. 2) does not have the cut which appears in (II.33).

The graph (Fig. 3) falls into the general class described by Fig. 4

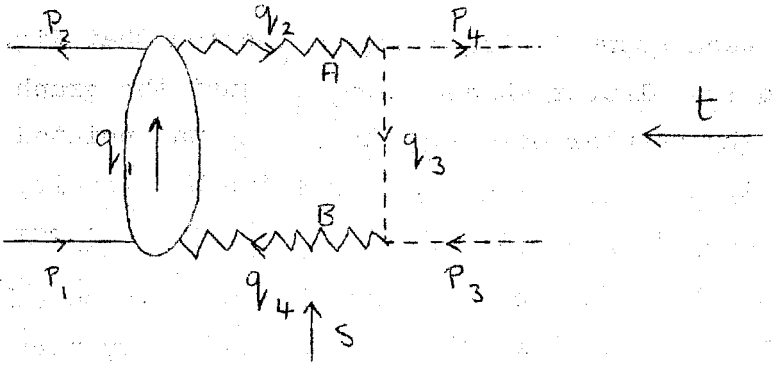

Fig. 4

where, in our particular case, the blob represents the cross (Fig. 5).

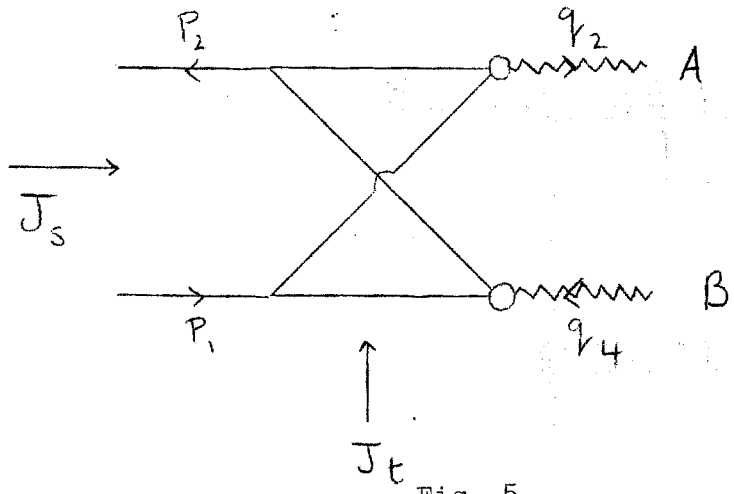

Fig. 5

The Regge poles A and B of Fig. 4 are associated with the scattering of $q_1-p_2 \to p_4+q_3$ and $q_3+p_3 \to q_1-p_1$, respectively. This description is not exact since A is really connected with some internal momenta of the blob, but it has all the correct analytic properties needed to illustrate the argument. Figure 4 may now be evaluated as a Feynman integral in the form

$$A(s,t) \sim \int \prod_i d q_i^2 \cdot J \cdot F(t, q_1^2, q_2^2, q_4^2) \cdot P_{\alpha(q_2^2)}(\cos\theta_A) \times \frac{B(q_2^2, q_3^2, m_x^2)}{|\vec{q}_3|} \times \frac{1}{(q_3^2 - m_x^2 + i\varepsilon)} \times \frac{B(q_4^2, q_3^2, m_x^2)}{|\vec{q}_3|} \cdot P_{\alpha(q_4^2)}(\cos\theta_B) \qquad \text{(III.1)}$$

where we are working in the centre-of-mass system of the t channel. There $B(W^2,a^2,b^2)$ is the residue function of a Regge pole of energy W connected to particles of "masses" a and b and $F(t,q_1^2,q_2^2,q_4^2)$ represents the amplitude of the blob. J is the Jacobian of the transformation of integration variables from d^4q_3 to $\prod_i d(q_i^2)$; θ_A, which is the scattering angle associated with the process $q_1-p_2 \to p_4+q_3$, may for our purposes be roughly represented by

$$\cos\theta_A \sim \frac{q_2^2 s + q_1^2 q_3^2}{q_1^2 q_3^2} \qquad \text{(III.2)}$$

and similarly

$$\cos\theta_B \sim \frac{q_4^2 s + q_1^2 q_3^2}{q_1^2 q_3^2} \qquad \text{(III.2')}$$

We may see from (III.2) and (III.2') that as $s \to \infty$, $\cos\theta_{A,B} \to \infty$ in part of the range of integration, unless q_1^2, q_3^2 also become suitably large over the whole range. We shall first show that whereas q_1^2 is somewhere bounded, q_3^2 can be made of the order of s by deforming the integration contour, so that $\cos\theta_{A,B} \sim O(1)$ as $s\to\infty$ and the Regge pole is never dominant. For this we have to know the singularity structure of the blob. In terms of the Mandelstam variables $J_s = (p_1-p_2)^2$, $J_t = (p_1+q_4)^2$ and $J_u = (q_4-p_2)^2$, the cross, Fig. 5, has only singularities of the type $J_t \equiv q_1^2 = 4m^2 - i\varepsilon$ and $J_u = 4m^2 - i\varepsilon$, but no explicit ones in J_s. From the relation

$$J_s + J_t + J_u = 2M_d^2 + q_2^2 + q_4^2 \qquad \text{(III.3)}$$

these points become

$$q_1^2 = 4m^2 - i\varepsilon$$

$$q_1^2 = (2M_d^2 + q_2^2 + q_4^2 - t - 4m^2) + i\varepsilon \qquad \text{(III.4)}$$

which may be put diagrammatically as in Fig. 6 :

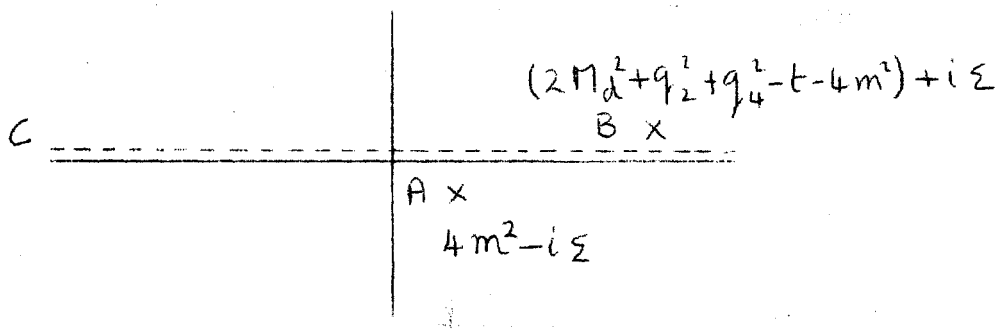

Fig. 6

where the original integration contour CD lies along the real axis. No matter what contour deformation is performed, the contour must cut the real axis between A and B and therefore must at some point have an s independent bound.

It is important to note that this type of argument is not restricted to the cross diagram: it holds for any blob which has both 2nd and 3rd double spectral functions. For it must then have singularities of the form $J_t = M_t^2 - i\varepsilon$, $J_u = M_u^2 - i\varepsilon$ and the previous discussion goes through unchanged.

If we had a cross on the right of the Regge poles as well, we could say that q_3^2 must be somewhere finite, no matter how the contour is deformed from which it follows that as $s \to \infty$, $\cos\theta_{A,B} \sim s$ and a Regge cut is produced. In other words, the lines q_2, q_3, q_5 of Fig. 2 would have, for part of the integration range, to be near their respective mass shells and so it is not surprising that this result is the same as UGM, who in effect take only the contribution exactly on the mass shells.

Before we examine in detail the q_3^2 integration, let us look at q_2^2 and q_4^2. From the kinematics, it is seen that both q_2^2 and q_4^2 must be negative and that as $q_2^2 \to \infty$, so must $q_4^2 \to \infty$. We now divide

the q_2^2, q_4^2 integration into finite parts where $\alpha(q_{2,4}^2) > \xi > \alpha(\infty)$ and the rest. If the Regge pole is built up from ladders, then $\alpha(\infty) = -1$ [11]. For the finite range integral, since the q_3 leg does not have a third double spectral function, there is no obvious reason why we cannot deform the q_3^2 integration. It can in fact be shown that all the singularities are of the form $q_3^2 = M^2 - i\xi$. We therefore deform the q_3^2 contour into the upper half plane a distance of the order of s until $\cos\theta_{A,B} \sim 1$ where the singularities of $\cos\theta_{A,B}$ interfere. From the study of the Bethe-Salpeter equation, it appears that $B(W^2, a^2, b^2)$ does not increase faster than logarithmically with a^2. Furthermore, since $|\vec{q}_3|$ behaves like q_3^2 for large q_3^2, this part of the integral is, ignoring logarithms, $O(s^{-3})$. We now consider the region where both q_2^2 and q_4^2 are large (note that one cannot be large without the other). It is found that we are not now able to deform the contours far enough and so there will be a fixed cut at $\ell = 2\alpha(\infty) - 1$, with an associated asymptotic behaviour $s^{2\alpha(\infty)-1}$. Since in this model $\alpha(\infty) = -1$, the whole amplitude for the graph is $O(s^{-3})$.

If the graph is looked at in the leading singularity approximation of Polkinghorne [13], the asymptotic behaviour obtained is $s^{-3} \log s$ [14].

It is important to consider what modifications of our assumptions would be needed to avoid this result, and whether these are reasonable. First, it was explicitly assumed that the residue function $B(W^2, a^2, b^2)$ does not increase as a power of the mass a for large a. While this seems reasonable from the Bethe-Salpeter equation, this is not a completely trustworthy dynamical model of the situation, because of the high mass intermediate states involved. In the evaluation of B in this way, only diagrams of type shown in Figs. 7.a,b are included

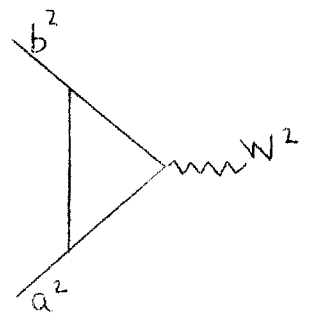

Fig. 7.a

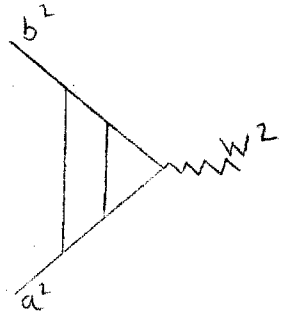

Fig. 7.b

that is, only those which satisfy two-particle unitarity in the W^2 channel. Consequently, diagrams like Fig. 7.c are neglected :

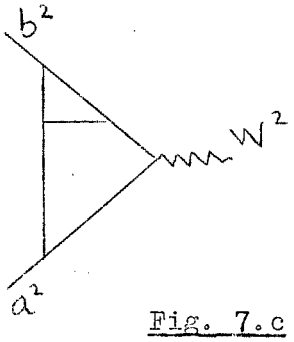

Fig. 7.c

It may be that as a^2 increases, the neglected graphs become more important to provide a power increase in B but we see no reason why this should be so.

A second possibility is that $\alpha(\infty)$ is greater than -1 due to the trajectory not going asymptotically to a negative integer. Since the argument described above would equally well hold if Regge cuts were substituted for poles in the xN amplitudes, $\alpha(\infty)$ would then refer to the leading cut and as such might well be greater than -1.

A third line of argument might be that even if the amplitude decreases asymptotically like s^{-3}, up to some energy higher than we have yet realized, it could actually be increasing. According to Mandelstam [4], the cut is cancelled by multi-particle unitarity effects and it is possible that not enough particles are produced at a given energy to give the cancellation. In terms of our previous discussion, we used the condition that in the finite range integration, L was small compared with s, (see Fig. 8)

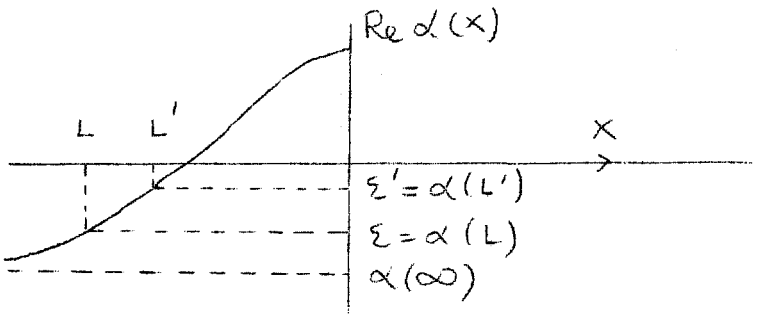

Fig. 8

where L is the limit of the q_2^2 integration. If s is not large enough for this to be true, then we must choose another value L' of L for which $s >> |L'|$. Doing this though allows the infinite integral from $L' \to \infty$, for which we cannot deform the contours, to induce a behaviour $s^{2\alpha(L')-1}$ instead of $s^{2\alpha(\infty)-1}$. However, although it is not possible to calculate $L' = L'(s)$, it would seem that $L'(s) = -s/10$ is on the conservative side and so above a few GeV, a fast decrease should still be expected unless $\alpha(\infty) = 1$, i.e., unless there is a fixed Regge cut at $\ell = 1$. This possibility cannot be excluded theoretically, but there may be experimental evidence that at the energies we are considering cuts are unimportant compared to Regge pole exchange [15),16)]. If the fixed cut does dominate x nucleon scattering, then the Glauber formulae (II.5), (II.6) and (II.7) contribute to the eclipse effect, (although the UGM form, of course, does not apply): on the other hand, if the fixed cut contribution is small compared to that of Regge pole exchange, then only the cut part of the elastic x nucleon amplitude is to be used in computing the eclipse correction to x deuteron scattering, which is therefore greatly reduced.

Thus the shadow term of UGM disappears at high energies, and there remains only the (perhaps much smaller) contributions of a fixed cut. We should like to suggest physically why this happens. The shadow term arises from the projectile x interacting with both the proton and neutron

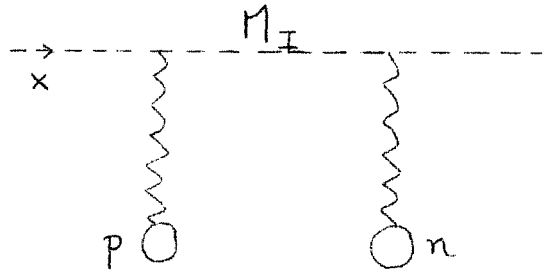

Fig. 9

We have shown that between the two scatterings the projectile has a very large mass M_I, but in the Regge model the nucleons are much more transparent to high mass objects. Hence Fig. 9 does not have a very large contribution.

IV. MODIFIED SHADOW TERM

From the results of Section III, it is seen that the shadow term corresponding to Glauber's model probably disappears very rapidly at high energies and that this is intimately connected with the non-appearance of Regge cuts in certain diagrams (Fig. 2). There remains the question of whether there exist diagrams which do exhibit a cut structure, other than those containing fixed cuts in the elementary processes, such that a more persistent eclipse term might exist. It will be shown that there do, but that they are associated with a subclass of inelastic intermediate states.

Consider the diagram in Fig. 10

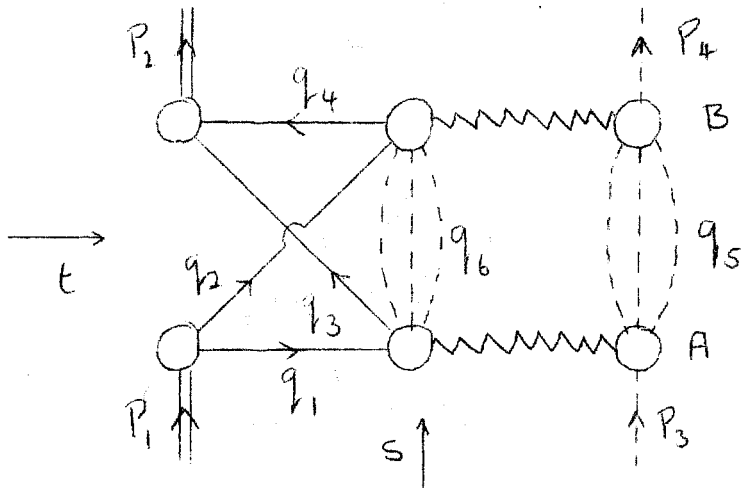

Fig. 10

The condition for the existence of such a cut in it was demonstrated in Section III to be that the subgraph, Fig. 11.a, must have singularities in the 2nd and 3rd spectral regions, e.g., be of the type Fig. 11.b

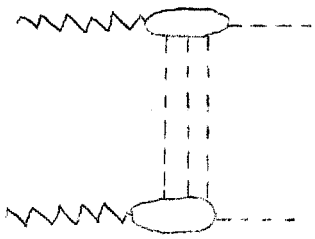

Fig. 11.a

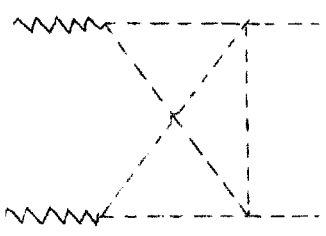

Fig. 11.b

Since the elastic graph, Fig. 2, is not of this form, then the Glauber formula cannot provide the dominant correction to the impulse approximation at high energies. However, let us for the moment forget this and calculate the contribution of Fig. 10 by using unitarity in the s channel in a similar manner to Section II. It can be written in the form of Fig. 10 where all the inelastic particles are put into two groups with masses $s_5^{\frac{1}{2}}$ and $s_6^{\frac{1}{2}}$ and momenta q_5 and q_6. This decomposition of the inelastic secondaries into two groups is seen experimentally. The dominant inelastic collisions at high energy show a jet structure. Considered in the c.m. system, we see the secondaries clustered together in two stronlgy collimated groups, moving in opposite directions. The masses of the jets $s_5^{\frac{1}{2}}$, $s_6^{\frac{1}{2}}$ are small compared with the incident particle momentum.

Let us first calculate the contribution of Fig. 10 to the unitarity relation when there are no inelastic events at the slow vertex, i.e., $q_6 \equiv 0$. Integrating over the invariant co-ordinates, cf. (II.26), we obtain

$$\mathrm{Im}\, A^{(e)}_{xd}(s,t) = \frac{-g^2}{(2\pi)^3}\int \frac{d^3q_2\, d^3q_3\, \delta^4(q_2+q_3+q_5-p_1-p_3)}{2E_2\ 2E_3\ (q_1^2-M^2)(q_4^2-M^2)} \times \frac{d^2q_5}{2E_5}\ A_p(s_a,t_a)\, A_n^*(s_b,t_b) \qquad \text{(IV.1)}$$

$$= \frac{-1}{M}\int d^3p\, G(p^2)\, A_p(s_a,t_a)\, A_n^*(s_b,t_b)\, \delta(q_5^2-s_5)\, \delta^4(p+q_5-p_1-p_3)\, d^4q_5$$

where as before $p = q_2+q_3$. Now, however, $A_p(s_a,t_a)$ refers to the inelastic amplitude of Fig. 12

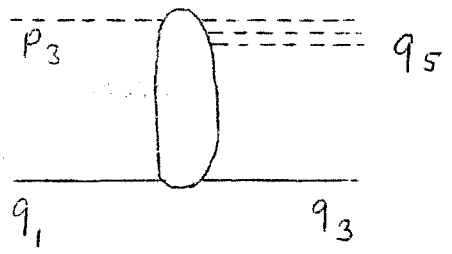

Fig. 12

where q_5 refers to a jet of small effective mass. If we now specialize to near the forward direction, the delta function in $(q_5^2 - s_5)$ limits p_z to be

$$p_z = \frac{s_5 - M_x^2}{2\omega} \qquad \omega \equiv |\vec{p}_s| \qquad \text{(IV.2)}$$

which tends to zero at high energies but at moderate energies has an important effect. From (IV.1) then we see that at the forward direction

$$\mathrm{Im}\, A^{(e)}_{xd}(s,0) \approx \frac{-1}{2\omega M}\int d^2p_\perp\, G(p^2)\, A_n^*\left(\tfrac{s}{2}, -p^2\right) A_p\left(\tfrac{s}{2}, -p^2\right) \qquad \text{(IV.3)}$$

where $p^2 = p_\perp^2 + p_z^2$ and p_z is determined by (IV.2). If we take the neutron and proton amplitudes to be the same, then A_N may be related to the total cross-section

$$\frac{d\sigma^T}{dt} = \frac{\pi^3}{M^2\omega^2} A^* A \qquad \text{(IV.4)}$$

Substituting this into (IV.3), we obtain :

$$\mathrm{Im}\, A^{(e)}_{xd}(s,0) = \frac{-M\omega}{2\pi^3}\int d^2p_\perp\, G(p^2)\, \frac{d\sigma^T}{d(-p^2)}\left(s/2, -p^2\right) \qquad \text{(IV.5)}$$

which by the optical theorem is

$$\sigma^{T(e)}_{xd} = \frac{-1}{\pi}\int d^2p_\perp\, G(p^2)\, \frac{d\sigma^T_{xN}}{d(-p^2)}\left(s/2, -p^2\right) \qquad \text{(IV.6)}$$

The Glauber formula (II.8) is obtained from (IV.6) by substituting $d\sigma^{el}_{xN}$ for $d\sigma^{T}_{xN}$ and remembering that in this case p_z is, by (IV.2), equal to zero. There is a further factor of 2 because there are two diagrams to be considered.

Let us now return to the study of Fig. 10 for the case when q_6 is non-zero. We show now that in most cases such graphs give a negligible contribution for purely kinematic reasons. From the mass shell condition on q_5, we obtain the relation

$$(q_6)_o = (P + q_6)_z \qquad \text{(IV.7)}$$

but since q_6 is on the mass shell as well

$$(q_6)_o^2 = s_6 + \vec{q}_6^{\,2} \qquad \text{(IV.7')}$$

Now a typical inelastic event has $\vec{q}_6 \sim s_6^{\frac{1}{2}} \sim 1$ GeV/c and so from (IV.7) $p_z = q_{6_o} - |\vec{q}_6| \gtrsim \sqrt{1+1} - 1 \approx 0.4$ GeV/c. But for p_z as large as this there is no contribution because the range of $G(p^2)$ is much smaller (~200 MeV/c). The case when only one pion is emitted at the slow vertex must be considered separately. Then $s_6^{\frac{1}{2}} = 0.14$ and with a pion momentum of, say, 0.3 GeV/c $|p_z| \sim 0.3(1-\cos\theta) + 0.03$ where θ is the angle between p and the z axis. We see therefore that although the pion graph can give contributions which fall inside the $G(p^2)$ peak, they are suppressed by a factor of about 1/10. We therefore claim that in accordance with (IV.6) the formula which obtains when the arguments of UGM are carried to their logical conclusion is

$$\sigma^{T(e)}_{xd} = \frac{-2}{\pi} \int d^3p\, G(p^2)\, \frac{d^2\sigma^{T}_{xN}(s_2, -p^2, s_5)}{d(-p^2)\,dp_z} \qquad \text{(IV.8)}$$

where σ^{T}_{xN} refers to the scattering of x and N to produce one slow recoil nucleon plus a jet of low effective mass $s_5^{\frac{1}{2}} \lesssim 3$ GeV; there is no inelasticity at the nucleon vertex. s_5 is given in terms of p_z by Eq. (IV.2).

In obtaining formula (IV.8) we have counted all diagrams of the type of Fig. 10, whether or not they have a Regge cut. However, using unitarity in the s channel can only be a good approximation when there is a cut in the appropriate diagram. In particular, since the elastic diagram (Fig. 2) was shown not to have one, we must discard from $d\sigma^{T}_{xN}$ the contribution $d\sigma^{el}_{xN}$, leaving only $d\sigma^{inel}_{xN}$. If we consider the case where the inelasticity takes the form of single pion production, then there are two types of diagram which contribute to (IV.8), [see Fig. 13]:

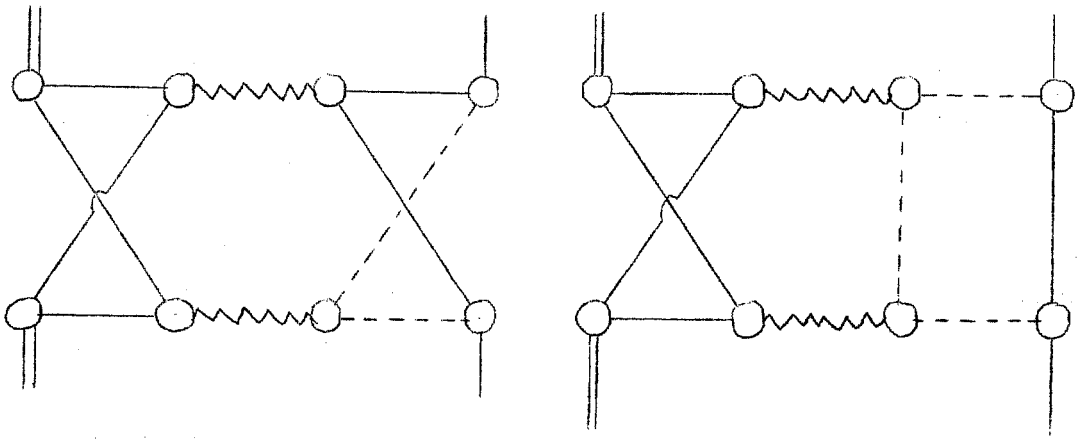

Fig. 13.a

Fig. 13.b

Figure 13.a showing a Regge cut while Fig. 13.b does not. If it is assumed that the diagrams have equal weight in the unitarity relation (which is not quite true), then the contribution of this type of diagram to σ^{T}_{NN} of (IV.8) is $\frac{1}{2}\sigma_{NN\to NN\pi}$. We can take into account the difference between the coupling of the Regge pole to the pions and nucleons by replacing $\frac{1}{2}$ by $\gamma(1) = 2\delta/(1+\delta)^2$ where δ is the relative coupling strength of the nucleons and pions. In double pion production, there are relatively more diagrams which have the required 3rd double spectral function and so this contribution to σ^{T}_{NN} is $\gamma(2)\times\sigma_{NN\to NN\pi\pi}$ where $\gamma(2) = (1+2\delta)^2/(2+\delta)^2$. In general

$$\gamma(r) = \frac{(r+2\delta-1)r}{(r+\delta)^2} \qquad \text{(IV.9)}$$

and has to multiply the cross-section for the production of r pions.

Of course many more things may happen such as strange particle production $NN \to NK\Lambda$. For this reason no simple formula of the Glauber type can be found. We are therefore forced to write the result of our derivation in the schematic form

$$\sigma_{xd}^{T(e)} = \frac{-2}{\pi} \sum_{A} \gamma(A) \int d^3p\, G(p^2)\, \frac{d^2\sigma_{xN\to AN}\left(s/2, -p^2, \mu^2\right)}{d(-p^2)\, dp_z} \qquad \text{(IV.10)}$$

where $p_z = (\mu^2 - M_x^2)/2\omega$. A is a state of effective mass μ which contains more than one particle and $\gamma(A)$ represents the probability of the existence of a cross in the appropriate diagram, Fig. 11.

Although we do not profess here a detailed evaluation of (IV.10), certain qualitative features can be discussed. It is, firstly, meant only as a high energy formula, since at low energies there will still be contributions from the non-cut terms. Assuming that we are at such an energy that these terms can be neglected, then we expect the shadowing to increase with energy. This follows because in general the total sum of inelastic events increases with energy as also does the multiplicity. However, the greater the number of particles in the state A, the closer is $\gamma(A)$ to unity, [cf., Eq. (IV.9)].

It should be stressed finally that the calculation of $\gamma(A)$ depends strongly upon whether the incident particle is pion or proton, but that in each case $\gamma(A) \to 1$ as the multiplicity increases.

V. REVIEW OF THE EXPERIMENTAL SITUATION

To what extent does the experimental evidence throw light on the correctness of our theoretical estimate of the eclipse effect ? We shall see in this Section that althcugh there is no conclusive evidence, the experiments which seem accurate enough to measure the shadow effect seem to indicate its persistence at high energies, with perhaps even a slight increase in magnitude.

The impulse approximation for scattering away from the forward direction contains the deuteron form factor $G(-t/4)$. Any estimate of this does not in general seem accurate to more than a few per cent, so that the most reliable information about the eclipse term must come from nearly forward scattering or from total cross-sections, since $G(0) \equiv 1$.

The experimental knowledge required involves the scattering or some particle x on protons, neutrons and deuterons. Since the proton is the only stable strongly interacting particle, the only case for which the necessary information can be directly obtained is where the particle x is a proton. Since free neutron targets are unavailable, we must measure the nx amplitude and then invoke time reversal to find the xn amplitude. The information for the proton is mainly limited by the absence of such direct n-p measurements. The results at high energies are confined to two Dubna experiments [17] at 5.5 and 8 GeV/c, whose quoted errors (~5%) make a determination of the shadow effect of the expected size impossible. In view of the precise information available on the p-p and p-d processes [18], further work with neutron beams would be particularly valuable, not only for the investigation of the shadow effect, but also as a direct check of the dominance of the exchange of $T = 0$ systems for small angles and high energies, an assumption we shall have to use below, because of the absence of np data.

For p-p and p-d scattering, accurate (~1%) measurements of total cross-sections are available up to 20 GeV/c and the p-p angular distributions near the forward direction have been carefully measured over this range under the stimulus of the Regge pole predictions [18].

The p-d angular information is not so complete but measurements have been made at Dubna of $p+d \to p+d$ with observation of the bound recoil deuteron over the range from 2.8 to 10.9 GeV/c [19]; at CERN a similar experiment at 19.3 GeV/c [20] included events in which the deuteron may disintegrate, and is thus harder to interpret from our point of view.

In the absence of accurate n-p measurements one is forced to make further assumptions. It is expected that at high energies the forward scattering will be dominated by $T = 0$ exchange in the crossed channel [21], so that apart from electromagnetic corrections, the p-p and n-p amplitudes will be the same. This conjecture is in agreement with the limited data available even at 5.5 GeV/c [17], though a difference of ~5% is not excluded. The principal contribution to the n-p/p-p difference will be ρ exchange. This has been estimated by Ahmadzadeh [22] using a Regge pole model that also fitted the charge exchange data. He found that $\sigma_{np} - \sigma_{pp}$ changes sign at 6 GeV and is around 2 mb at 10 GeV, above which it decreases slowly to zero. When compared with the experiments on total cross-sections, these results favour a fairly constant shadowing up to 20 GeV.

If we pass to the system for which the incident particle x is a pion, we find a much more decisive experimental situation, although its analysis involves further assumptions. Whereas $\pi^{\pm} n$ scattering cannot be measured, charge symmetry says that apart from electromagnetic effects the amplitudes should be equal to those for $\pi^{\mp} p$. Galbraith et al. [23] measured the total cross-sections for π^+ and π^- on protons and deuterons from 6 to 20 GeV/c. After the removal of the Coulomb scattering, they found a shadow effect

$$\rho = 2\,\frac{\sigma^T_{\pi^+ p} + \sigma^T_{\pi^- p} - \sigma^T_{\pi^+ d}}{\sigma^T_{\pi^+ p} + \sigma^T_{\pi^- p}} \qquad (V.1)$$

of the order of 8 or 9% with a slight tendency to rise towards the higher energies. However, the statistical errors are around 3%.

A similar conclusion was reached by Baker et al. [24] at somewhat lower energies, but at 5.6 GeV/c their screening factor ρ was only 5%. While it is just possible that this discrepancy is within the quoted errors, it is a possible indication that the effect is actually increasing with energy.

The difficulties in the interpretation of these results are mainly associated with the removal of electromagnetic effects. There is firstly the Coulomb interaction. In Eq. (V.1) only the combination $(\sigma_{\pi^+p}+\sigma_{\pi^-p})$ enters so that to first order in e^2 there is no effect. The only other quantity entering in (V.1) is σ_{π^+d}, but since experimentally this was found to be closely equal to σ_{π^-d}, where the Coulomb effect has the opposite sign, it may be assumed that the Coulomb effect has no appreciable influence on the measured value of ρ. Incidentally, the equality of σ_{π^+d} and σ_{π^-d} has been interpreted as showing the validity of the charge symmetry of the pion-nucleon force at high energies [23]. We should like to stress that this is only a very limited check. If, as seems plausible, these amplitudes are dominated by the exchange of $T=0$ systems in the crossed channel ($T\neq 0$ is forbidden because the deuteron has $T=0$), we are in fact only checking charge conjugation. That is, the amplitudes of Figs. 14.a,b are equal by charge conjugation since x^o must be self-conjugate.

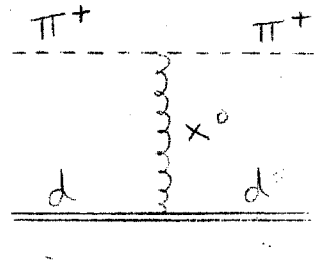

Fig. 14.a

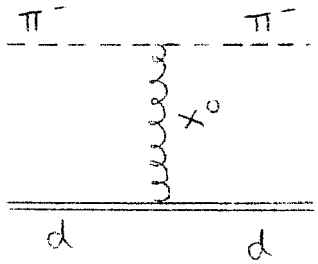

Fig. 14.b

On the other hand, we expect a difference between $\pi^- n$ and $\pi^+ p$ even if both processes are dominated by t channel singularities, because of the difference between the proton and neutron electromagnetic properties in such diagrams as Figs. 15a,b :

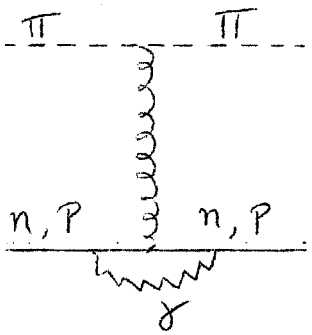

Fig. 15.a

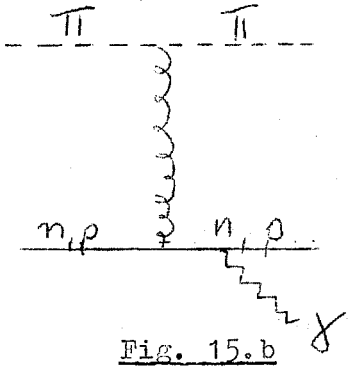

Fig. 15.b

These are not easily calculable but it seems likely that they will be down by a factor of order $\alpha \sim 1/137$ from the non-electromagnetic terms and so a small effect is not excluded. We know of no other experiment which rules out a violation of charge symmetry of this order of magnitude at these energies, although the effect may be much smaller. In summary then, it is not expected that violations of charge symmetry will invalidate the results obtained from (V.1), but it is possible.

After the shadow effect has been determined experimentally, it is of interest to compare it with our formula (IV.10). The experimental quantities appearing in this are not as easy to measure as those required in the Glauber formula. The information that is required refers to cross-sections for the processes $x+N \to A+N$ where A is a system of at least two particles, but with low effective mass $\mu \lesssim 3$ GeV/c. The data is required for small momentum transfer to the recoil nucleon, and no slow particles should be emitted with the nucleon. Not only is the distribution in momentum transfer required, but also the distribution in effective mass μ, and preferably knowledge of what the constituents of the state A are.

Possibly the simplest type of experiment which will determine most of the parameters involves a missing mass determination. If, in nucleon-nucleon scattering at ~20 GeV, the momenta of the initial and final fast nucleon are measured then both the momentum transfer t and the effective mass μ of all other outgoing particles may be calculated. Only events with μ less than, say, 3 GeV should be accepted to avoid the possibility of particles being emitted from both vertices. In the process described above, the particles are actually emitted at the slow vertex, but by Lorentz invariance the cross-section is the same as that for the case when they are emitted at the fast vertex. Of course in this type of experiment, since no investigation of what constitutes the state A is made, it is correspondingly difficult to measure $\gamma(A)$. Such experiments have been carried out at CERN [25] down to 2 mrad and at momenta 10, 19.3 and 26.4 GeV/c. We confine ourselves to a simple estimate of the size of the shadow term that we predict from this data. We shall take the inelastic cross-section cut-off at a mass of the inelastic system such that $p_z = (s_5 - M_N^2)/2\omega = 0.1$ GeV/c, giving a cross-section at 19.3 GeV/c, $d\sigma/dt$ of the order of 25 mb/GeV^2/c^2 and a shadowing in p-d scattering of $100\langle r^{-2}\rangle\gamma$ where $\langle r^{-2}\rangle$ is in GeV/c^2. This is probably consistent with the data but on the small side.

VI. SUMMARY AND CONCLUSIONS

The main aim of the present work was to examine critically the evaluation of the shadow term which appears in the scattering of high energy particles from deuterons. It appears that the main result is to cast grave doubts on the methods of extracting neutron data from deuteron data at high energies. In the language of complex angular momenta, if the amplitude for the scattering of a projectile x off a nucleon is parametrized by a Regge pole exchange, then the Glauber form for the x deuteron amplitude has a Regge cut; however, a complete evaluation not relying on the unitarity approximation shows that they lie at $\ell = 2\alpha(\infty) - 1$ rather than at the originally predicted position $\ell = 2\alpha(t/4) - 1$. In the high energy limit we therefore expect to have very little trace of such terms.

It was shown in Section IV that there is another set of diagrams which contribute to the x-d amplitude and which do have a cut at $\ell = 2\alpha(t/4) - 1$. In Eq. (IV.10) we have attempted an evaluation of the contribution of such cuts. This formula is more complicated than the equivalent formula of Glauber, but in principle the quantities entering in it are measurable or estimatable. In addition to high energy cross-sections, etc., there appears the deuteron form factor $G(p^2)$ and more reliable estimates of this are needed. From a preliminary look at the data, it would appear that the shadow term (IV.10) is too small, but this must be checked by detailed calculation and measurement. If we are at an energy where the non-Regge-cut terms may be neglected, we predict that the shadowing will increase with energy, essentially because both total inelastic cross-sections and multiplicities increase with energy. Some increase with energy is indeed seen from the pion data.

We should like to stress again the importance of an accurate theory of shadowing, well checked by experiment. The high energy experiments are now achieving accuracies which make possible cross-section determination to better than 1% so that the estimate of the shadow term is now the limiting factor in fixing the neutron cross-sections. Accurate experimental results with high energy neutron beams are now absolutely essential to check the theoretical estimates and allow their extension to other scattering processes.

Finally, it is amusing to note that if the present measurements of an approximately constant shadow term at high energy are accepted, it constitutes the first manifestation of a Regge cut to be observed experimentally, independently of the details of the theory we have presented. Whereas we expect Regge cut terms to be important in the proton-proton amplitude itself, they are there difficult to disentangle from the Regge pole contributions.

ACKNOWLEDGEMENTS

We should like to thank G. Cocconi and A. Wetherell for several enlightening discussions, and D. Amati, T. Ericson and A. Martin for useful comments. A useful correspondence with A.R. Swift is also acknowledged. Dr. G.H. Stafford supplied us with valuable information from the Rutherford Laboratory p-p experiments. One of us (C.W.) is grateful to E. Schönlank for an engaging proposal. Two of the authors (E.S.A. and V.L.T.) would like to thank Professor L. Van Hove for the kind hospitality of the Theory Division of CERN.

REFERENCES

1) M. Gell-Mann, CERN seminar, July 1965 (unpublished).

2) R.J. Glauber, Phys.Rev. 100, 242 (1955).

3) B.M. Udgaonkar and M. Gell-Mann, Phys.Rev.Letters 8, 346 (1962). This paper will be called UGM.

4) S. Mandelstam, Nuovo Cimento 30, 1127 and 1148 (1963).

5) D. Amati, S. Fubini and A. Stanghellini, Nuovo Cimento 26, 896 (1962).

6) See, for instance, R.G. Sachs, "Nuclear Theory", p. 79 [Addison-Wesley, Cambridge, Mass., 1953].

7) For a full discussion on the connection between form factors and wave functions, see :
R. Blankenbecler and L.F. Cook, Phys.Rev. 119, 1745 (1960).

8) R.E. Cutkosky, Proceedings of the 1960 High Energy Conference (Rochester, 1960), p. 236.

9) J.J. Brehm and J. Sucher, Ann.Phys. (New York) 25, 1 (1963).

10) F. Gross, "Relativistic Treatment of Loosely Bound Systems in Scattering Theory", Cornell preprint, June 1965.

11) B.W. Lee and R.F. Sawyer, Phys.Rev. 127, 2266 (1962).

12) C. Wilkin, Nuovo Cimento 31, 377 (1964).

13) J.C. Polkinghorne, J.Math.Phys., April 1963.

14) A.R. Swift, private communication.

15) R.J.N. Phillips and W. Rarita, Lawrence Radiation Laboratory report UCRL 16097 (1965), to be published.

16) G.F. Chew, CERN seminar, August 1965 (unpublished).

17) L. Ozhdanji, V.S. Pantuev, M.N. Khachaturyan and I.V. Chuvilo, Soviet Physics (JETP) 15, 272 (1962);
M.N. Khachaturyan and V.S. Pantuev, Soviet Physics (JETP) 18, 1239 (1964).

18) See, for example, G. Belletini, G. Cocconi, A.N. Diddens, E. Lillethun, J. Pahl, J.P. Scanlon, J. Walters A.M. Wetherell and P. Zanella, Phys.Letters 14, 164 (1965), and
R.F. George, K.F. Riley, R.J. Tapper, D.V. Bugg, D.C. Salter and and G.H. Stafford, Rutherford Laboratory preprint, 1965; as as well as References 23) and 24). Earlier work on total cross-sections is reviewed in Diddens et al., Phys.Rev.Letters 9, 32 (1962).

19) L. Kirillova et al., Dubna preprint E-1820 (1964).

20) CERN experiment 1965, G. Cocconi and A.M. Wetherell (private communication).

21) D. Amati, L.L.Foldy, A. Stanghellini and L. Van Hove, Nuovo Cimento 32, 1685 (1964).

22) A. Ahmadzadeh, Phys.Rev. 134, B633 (1964).

23) W. Galbraith, E.W. Jenkins, T.F. Kycia, B.A. Leontic, R.H. Phillips, A.L. Read and R. Rubinstein, Phys.Rev. 138, B913 (1965).

24) W.F. Baker, E.W. Jenkins, T.F. Kycia, R.H. Phillips, A.L. Read, K.F. Riley and H. Ruderman, Proceedings of the Sienna Conference on Elementary Particles, 1963. Ed. by G. Bernardini and G. Puppi (Società Italiana di Fisica, Bologna, 1963).

25) G. Belletini, G. Cocconi, A.N. Diddens, E. Lillethun, J.P. Scanlon, A.M. Shapiro and A.M. Wetherell (to be published in Phys. Letters).

FIGURE CAPTIONS

Figure 1 Diagram for the impulse approximation to x-d scattering.

Figure 2 Diagram for Glauber's eclipse correction to x-d scattering, with cut $\alpha - \beta$ giving three-particle intermediate state contribution.

Figure 3 Example of a contribution to the imaginary part which was omitted in the calculation of Section II.

Figure 4 General class of graphs to which theorem of Section III applies.

Figure 5 Particular case of Fig. 4 corresponding to Fig. 2.

Figure 6 Location of singularities in the q_1^2 plane.

Figure 7 Examples of diagrams included in Bethe-Salpeter equation theory of Regge pole vertices [diagrams a) and b)]. Diagram c) is an example of one which is not included.

Figure 8 Typical positions of L and L'.

Figure 9 Contribution of high mass intermediate states.

Figure 10 Inelastic intermediate state contributions to eclipse effect.

Figure 11 The subgraph a) must be of the type b) to contribute to the eclipse effect.

Figure 12 Inelastic x nucleon amplitude.

Figure 13 Contribution to eclipse effect from one-pion production.

Figure 14 Diagrams for π-d scattering.

Figure 15 Diagrams for π-N scattering.